minerals

MDPI

Article

Setting Time of Alkali-Activated Binders Exposed to Co-60 Gamma Radiation

Luka Rubinjoni [1,*], Srboljub Stanković [2] and Aco Janićijević [3]

[1] Insitute of General and Physical Chemistry, Studentski trg 12/V, 11000 Belgrade, Serbia
[2] Vinča Institute of Nuclear Sciences, University of Belgrade, Mike Petrovića Alasa 12–14, 11001 Belgrade, Serbia; srbas@vin.bg.ac.rs
[3] Faculty of Technology and Metallurgy, University of Belgrade, Karnegijeva 4, 11000 Belgrade, Serbia; janicaco@tmf.bg.ac.rs
* Correspondence: rubinjoni@tmf.bg.ac.rs

Abstract: An investigation of the effect of gamma radiation was carried out on the setting time of alkali-activated binder paste. Mechanically activated coal fly ash (FA), ground granulated blast furnace slag (BFS), and their 1:1 mass mixture (MIX) were activated by water glass with a module of 1.5. Fresh paste was cast into molds and exposed to Co-60 gamma radiation, at a dose rate of 9.62–9.53 Gy/h, until the final setting. The initial and final setting times were determined by measuring the penetration of the Vicat needle at regular intervals. The initial setting times were 1 h 3 min for BFS, 1 h 55 min for MIX, and 3 h 28 min for FA. The final setting times were 1 h 10 min for BFS, 2 h 13 min for MIX, and 4 h 1 min for FA. The received doses were 8.02 Gy for BFS, 17.54 Gy for MIX, and 34.14 Gy for FA. Exposure to gamma radiation resulted in a shorter initial setting time for BFS, a shorter final setting time for FA, and results with an insufficiently visible impact on MIX. For dose rates in the 9–10 Gy/h range, the irradiation by Co-60 gamma rays during setting did not lead to flash, nor did it delay the setting of alkali-activated binder pastes.

Keywords: gamma radiation; geopolymer; setting time; alkali-activated binder; fly ash; ground granulated blast furnace slag

check for updates

Academic Editors: Dariusz Mierzwiński and Wei-Ting Lin

Received: 30 September 2024
Revised: 8 November 2024
Accepted: 25 November 2024
Published: 28 December 2024

Citation: Rubinjoni, L.; Stanković, S.; Janićijević, A. Setting Time of Alkali-Activated Binders Exposed to Co-60 Gamma Radiation. *Minerals* **2025**, *15*, 25. https://doi.org/10.3390/min15010025

Copyright: © 2024 by the authors. Licensee MDPI, Basel, Switzerland. This article is an open access article distributed under the terms and conditions of the Creative Commons Attribution (CC BY) license (https://creativecommons.org/licenses/by/4.0/).

1. Introduction

The safe, reliable and affordable management of radioactive and nuclear wastes is one of the main challenges for the current and future use of nuclear technologies. Materials based on inorganic binders (cement, grout, mortar, and concrete) are used both as construction materials and as direct constituents of stabile waste forms [1]. The most commonly used material in construction is ordinary Portland cement (OPC), with a long history of use and (comparatively) well-studied behavior in radioactive and nuclear applications [2]. To overcome some shortcomings of OPC in waste conditioning, alternative binders are under development [3]. One such class of materials are alkali-activated binders, formed through the reaction of fine aluminosilicate powders with strong alkaline solutions (activators) [4]. The terminology in the field varies: alkali-activated binders with low calcium content are called geopolymers; binders with significant calcium content are usually referred to by other names, but are included in geopolymers by some authors [5]. The binding phase of geopolymers is an alkali aluminosilicate gel, with aluminum and silicon linked in a three-dimensional tetrahedral gel framework that is relatively insoluble in water. If calcium is present in the powder, it will participate in the matrix as calcium silicate hydrate [6]. Powders with different calcium contents can be mixed, and activator traits such as the

modulus and alkalinity can be adjusted to obtain matrices with desirable characteristics: setting times and flows that are practical for the planned application, and high mechanical resistance and retention (low leaching) of radionuclides [7]. The process of alkali activation starts with the partial dissolution of aluminosilicates though the breaking of Si-O-Si bonds by OH^- ions, followed by cross-linking and polymerization by forming new Si-O-Si bonds, and ending with the precipitation of the cross-linked particles [4].

A multi-scale review of the effects of gamma radiation on Portland cement-based concrete is given by Reches, considering dry-cask nuclear waste storage as the use case [8]. The prominent effect of high dose rates of gamma radiation on cement-based materials is radiogenic heating, bearing a negative effect on the mass, dimensional soundness, and mechanical properties of cement products in a manner comparable to conventional heating. When Portland cement-based concrete is heated, the water found in the pores and bound in the cement hydrates is gradually lost. The dehydration of ettringite is completed by 120 °C, the dehydration of calcium silicate hydrate (C-S-H) proceeds approximately linearly over the range of 120–800 °C, and the dehydration of $Ca(OH_2)$ proceeds approximately linearly over the range of 400–530 °C. The resulting shrinkage of cement paste and thermal expansion of concrete aggregates causes microstructural stresses and cracks that propagate from aggregate surfaces, leading to a decrease in the strength and modulus of elasticity. During use, the dry casks are constantly heated by the encased fuel and exposed to variation in external/atmospheric conditions, potentially leading to cumulative crack development over multiple heating/cooling, dehydration/rehydration, and even freeze/thaw cycles. Other potentially relevant mechanisms of gamma ray/concrete interaction include the dislocation of atoms in cementitious phases, breaking of covalent bonds, radiolysis of water, dehydration of cement hydrates, and amorphization of aggregates. Gamma photons can carry enough energy to dislocate atoms in the cement paste, which consists primarily of amorphous C-S-H. Such dislocations do not change the fundamental structure of the binder paste, but can affect the porosity, reducing the volume of micro- and mesopores. Even without dislocating atoms, ionizing radiation may break covalent bonds and create radicals, leading to cross-linking of the C-S-H polymers and embrittlement of the bulk structure [8]. Water is radiolyzed in a set of reactions called the Allen cycle, yielding H_2 and H_2O_2 through a number of intermediate ionic (H^+, OH^-) and radical (e-aq, H*, OH* etc.) species. Bouniol and Aspat have recognized the formation of H_2O_2 as particularly important, as it may react with $Ca(OH)_2$ and H_2O to form $CaO_2 \times 8H_2O$ (calcium peroxide octahydrate), which rapidly carbonates into $CaCO_3$ in the presence of CO_2 [9]. Carbonization leads to the decrease in the pH of the binder, which may contribute to the de-passivation and corrosion of steel reinforcement commonly present in concrete structures. The pore structure is refined due to the buildup of $CaCO_3$, leading to a reduction in total porosity and mass transfer rates, which reduces the leaching and ingress of aggressive species, but can impede the exhalation of hydrogen and other gasses. Carbonation increases the strength and modulus of elasticity of cement because $CaCO_3$ has higher stiffness and hardness compared to $Ca(OH)_2$, but can lead to shrinkage and cracking because $CaCO_3$ has a smaller specific volume. Irradiation-induced carbonation was not identified in Portland cement blends with high BFS loadings (9:1 ratio of BFS to PC) [10]. The radiolysis of water can lead to the dehydration of C-S-H and $Ca(OH)_2$, displaying effects similar to those of dehydration by heating even in the absence of significant radiogenic heating of the material [8]. The presence of iron species disrupts the recycling of H_2 in the Allen cycle, and leads to excess production of hydrogen gas, which can negatively impact the waste form through the excision of pore water, weakening of the cement matrix, and the buildup of flammable/explosive gas [11]. Gamma radiation interacts with aggregates and additives of concrete, potentially causing

dislocations of atoms in crystal lattices, leading to the amorphization of SiO_2-rich materials such as quartz [8].

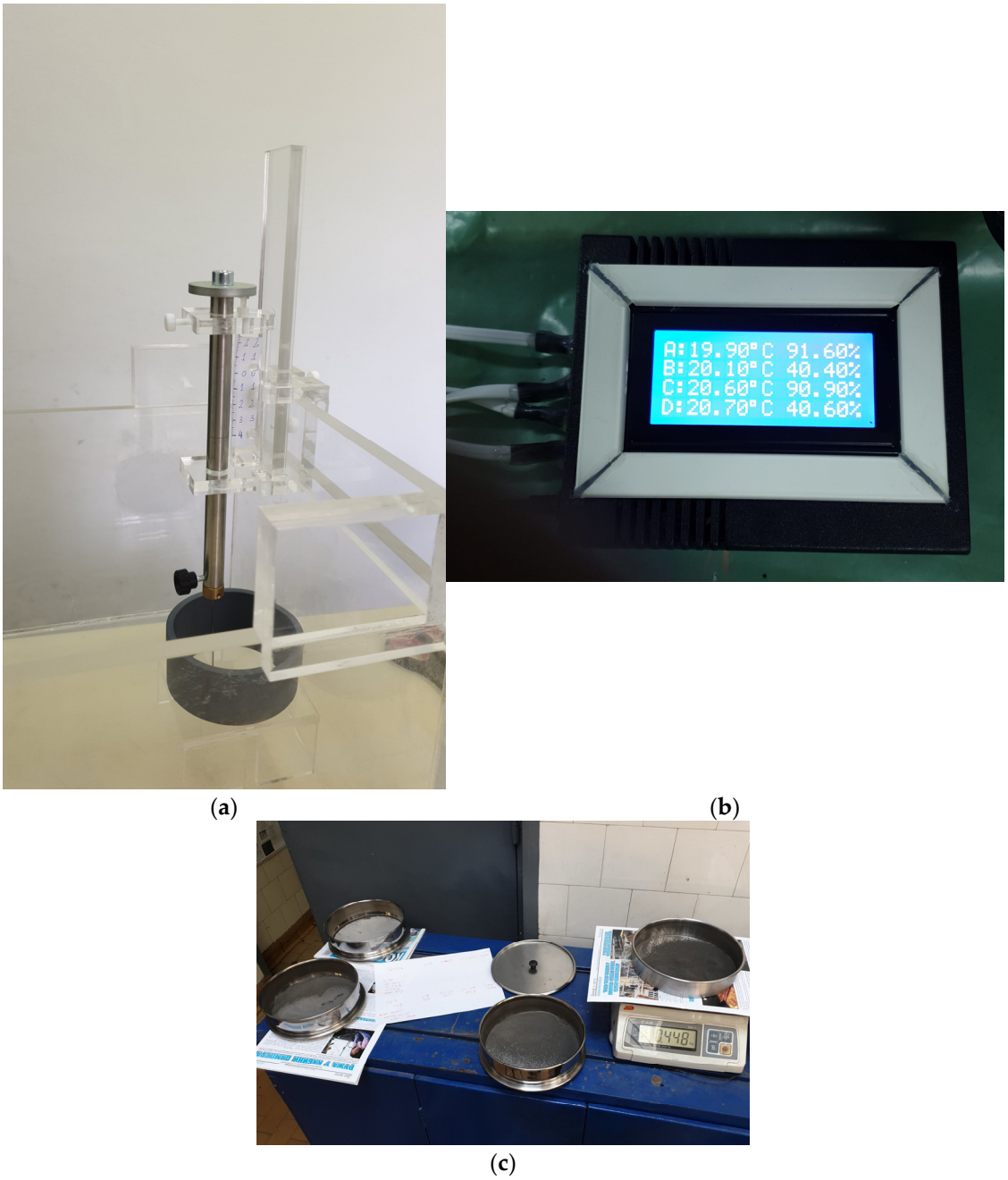
The effects of gamma radiation on alkali-activated binders, in the context of their applicability for radioactive waste treatment, were reviewed by Cantarel et al. in 2017, and Phillip et al. in 2023 [12,13]. Direct comparisons of the published primary research results are complicated by high variance in the selected base materials (aluminosilicate powders and activators) and irradiation protocols (sources, dose rates, doses, curing and aging of the material before and after the irradiation, etc.) and the observed effects (changes in compressive strength, microstructure, release of hydrogen due to radiolysis of water, etc.). The general conclusion is that alkali-activated binders perform as well as OPC-based ones, or outperform them. When exposed to a dose rate of 600 kGy/h, the radiolytic yield of hydrogen is dependent on the molar ratio of water in the geopolymer sample, observed to be in the 0.9×10^{-8} to 1.13×10^{-8} mol/J range for sealed (water-saturated) samples, and about 6×10^{-9} mol/J for samples stored in air [14,15]. Under this irradiation regime, an increase in compressive strength of about 10% was observed after exposure to a dose of 1 MGy. Gamma irradiation had an effect on porosity, increasing it from 7 nm (non-irradiated control) to a range of 10–50 nm (irradiated sample). Pair distribution function analysis showed only a slight shift decrease in Si-O-Si bridging, indicating that gamma irradiation induces slight densification of the geopolymer but does not significantly modify its amorphous structure [15]. Chupin et al. further explored the radiolytic yields of geopolymers, confirming the high correlation between the water content and radiolytic yield of hydrogen, and highlighting the importance of a binder's porous structure and the effect of the type of activator (sodium-, potassium-, or cesium-based). When the average pore size decreased, the larger specific surface area provided a larger solid/liquid interface for the release of secondary electrons upon gamma irradiation [16]. Geddes et al. reported a significant loss of free water from metakaolin geopolymer formulations upon gamma irradiation, with an increase in porosity and notable carbonation, but with minimal changes in the main binder gel phase under received doses up to 1 MGy [17]. Yeoh et al. investigated the long-term gamma irradiation effects on the mineralogical, microstructural, structural, physical, and chemical properties of 40 wt% blast furnace slag +60 wt% fly-ash geopolymer pastes. Two competing effects were identified: beneficial equilibration at initial lower dosages, which enhanced gelation and crosslinking, and detrimental equilibration at higher dosages, causing structural and microstructural destabilization. The transition where detrimental equilibration begins to dominate occurred at a dosage of about 4 MGy, after approximately five months of irradiation. The compressive strength of the binder increased from ~57 MPa to ~83 MPa (approximately a 45% increase) after two months of irradiation and a dose of 1574 kGy. Even with the effects of detrimental equilibration, the compressive strength of the irradiated sample after 6 months and a received dose of 4822 kGy remained at ~64 MPa, exceeding the control sample's ~58 MPa. Gamma radiation enhances curing through the conversion of less crosslinked silicate species Q^0, Q^1, and $Q^{1'}$ to more crosslinked Q^2, Q^3, and Q^4. As the received dose increases, new Si^{4+}, Al^{3+}, and Ca^{2+} ions are released from unreacted BFS, FA, and present minerals, which further enhances geopolymerization, but Q^4 species are converted to Q^0 and Q^2 (less ordered silicate species). Geopolymer pastes remained resistant to leaching under irradiation, emphasizing their potential for the immobilization of intermediate-level waste [18]. Alkali-activated binders are heat-resistant materials, making radiogenic heating inherently less of an issue, compared to OPC materials. Geopolymers retain significant compressive strength even after exposure to temperatures of 1000 °C, and outperform OPC in freeze/thaw tests [19,20].

The three most common use scenarios for cement-based materials in radioactive waste management are the production of structural elements and containers; cementation—the direct mixing of radioactive waste and grout/mortar; and the encapsulation of dried and compressed containers containing waste. In the first scenario, the material is prepared and cast before any exposure to radioactive waste, it has time to solidify and cure, and any additional operations can be performed before the introduction of waste. In the second scenario, the waste is mixed with freshly prepared, flowing grout or mortar, which allows the waste to react chemically with the binder matrix as it solidifies and cures, and exposes the nascent matrix to ionizing radiation. The chemical composition of the waste changes as a result of radioactive decay, possibly leading to new interactions with the solidified matrix [21]. Depending on the activity of the waste, the radiolysis of water and development of hydrogen in the material can have detrimental effects on the waste form [22]. In the third scenario, containers with radioactive waste (steel drums being the standard) are dried, compressed (either by compacting the waste inside the steel drum, or compacting the entire drum containing the waste), deposited in a larger container (either a pre-cast concrete vessel, or a larger steel drum), and grouted [23]. In this case, there is a barrier between the cementitious matrix and radioactive waste, preventing chemical contact and absorbing alpha and beta particles. The nascent matrix is exposed to gamma radiation from the waste as it solidifies.

The main topic of research for the use of alkali-activated binders in radioactive waste management has been the chemical interactions (with a focus on leaching) and long-term effects of ionizing radiation. In order to avoid radiation protection issues and reduce costs, cementation experiments are often performed with simulants—radiostable isotopes of elements commonly present in radioactive waste [24]. The long-term effects of ionizing radiation are studied by estimating the total dose the matrix is exposed to during radioactive decay of the waste, and exposing the material to such a dose at higher dose rates, so that the experiment can be completed in a practical time-frame [17,18]. Rheological properties are studied both to gain insights into the process of matrix formation and to meet the practical demands of the waste form [25]. The fresh binder must maintain proper flow during mixing and pouring, and then set, which will lead to long-term solidification of the matrix and optimal mechanical traits. Binder setting time is a robust and easily applicable measure of time needed for a phase change in binder paste. The initial setting time indicates the beginning of the solidification of the gel. The final setting time indicates the end of workability of the binder—the point in time in which the paste completely loses its plasticity [26]. The binder setting times of alkali-activated binders show a lot of variation compared to Portland cement—from significantly shorter times characteristic of calcium-rich binders to prolonged times of low-calcium binders [27]. Setting times that are too short or too long are indicative of suboptimal matrix design and pose practical problems. Flash setting occurs when the matrix solidifies before mixing and casting is complete, effectively halting the operation. Delayed setting occurs when the binder takes a long time to set, or does not set at all, and yields a material with poor mechanical and chemical properties. The effects of ionizing radiation on the setting times of cement pastes have rarely been investigated. To the authors' knowledge, the irradiation of fresh Portland cement paste and measurement of setting times were conducted by B. Nowakowski in 1972 [28,29]. Authors have performed exploratory experiments on irradiating fly-ash geopolymer binder [26]. The effects of gamma radiation on binder setting times for binders prepared from fly ash, ground granulated blast furnace slag, and their mixture, with sodium water glass as the activator, are presented in this paper.

2. Materials and Methods

Fly ash was obtained from the "Nikola Tesla B" thermoelectric power plant (Obrenovac, Serbia) in February 2022. This ash is a mixture of particles collected in four cascaded electrostatic flue gas filters (the "composite"), and as such, is either utilized in the production of Portland cement or deposited on ash heaps. Granulated blast furnace slag was obtained from "HBIS" steel works (Smederevo, Serbia) in May 2022. The slag is utilized in the production of Portland cement, and is ground at cement plants. For this experiment, the slag was ground in a ringed vibration mill. The same device was used for mechanical activation of the composite fly ash. The particle sizes of the resulting powders were determined by dry-sieving (depicted in Figure 1c), as presented in Table 1.



(**a**) (**b**)

(**c**)

Figure 1. (**a**) The Vicat piston and needle on the carrier/bridge, positioned over the mold in the acrylic chamber; (**b**) an Arduino device showing the readings of the four DHT22 sensors; (**c**) measuring the weight of the powder fractions after dry-sieving.

Table 1. Particle sizes for FA and BFS.

>100 µm	63–100 µm	45–63 µm	<45 µm	
4%	17%	29%	50%	FA
4%	10%	21%	65%	BFS

The chemical composition and loss on ignition (LOI, at 950 °C) for FA and BFS were determined at the Institute of Mining, Belgrade, and are presented in Table 2.

Table 2. Chemical composition and LOI for FA and BFS [w%].

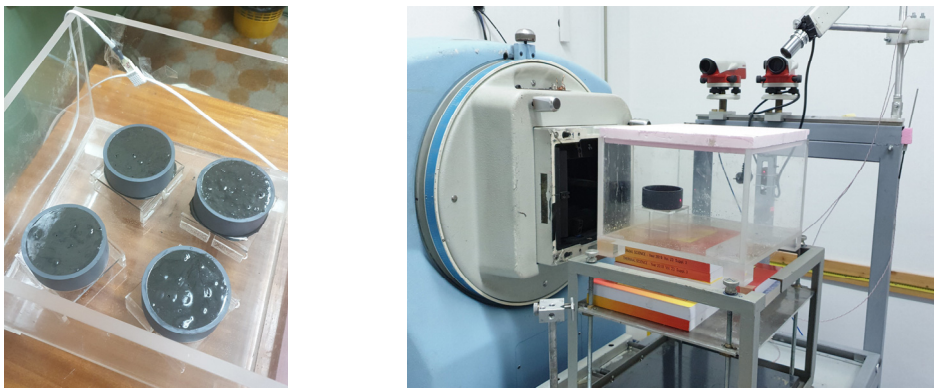
LOI	K_2O	Na_2O	TiO_2	P_2O_5	SO_3	MgO	CaO	Al_2O_3	Fe_2O_3	SiO_2	
3.49	1.44	0.61	1.04	0.02	1.10	1.10	3.93	25.52	6.19	55.54	FA
0.74	0.95	0.85	0.85	0.01	2.42	2.42	29.05	2.55	0.26	38.80	BFS

Sodium water glass was procured from "Galenika Magmasil", Belgrade (module s = 2.07; Na_2O w% = 13.3; SiO_2 w% = 26.7). The module and concentration of the activator were adjusted to s = 1.5 and Na_2O w% = 10 using deionized water and granulated NaOH. The activator/powder ratio was optimized to achieve flow in the range of 120–160 mm, tested on an EN 1015-3 cement flow table. The paste compositions are presented in Table 3.

Table 3. Paste compositions: mass of slag, ash, and activator; activator/powder ratio (A/P); water/solid ratio (W/S); and flow.

Flow [mm]	W/S	A/P	Activator [g]	Ash [g]	Slag [g]	
125	0.21	0.3	180	0	600	BFS
137	0.37	0.55	275	250	250	MIX
155	0.52	0.8	360	360	0	FA

A pair of acrylic climate chambers were constructed to maintain the irradiated and control samples at a steady temperature and relative humidity during setting [30]. The chambers were partially filled with water and closed with polystyrene lids. Sample holders/mold bottoms were constructed to keep the paste molds above the water surface. A bridge/holder for the Vicat piston and needle was constructed to enable the measurement of penetration without removing the sample from the chamber, as depicted in Figure 1a. An Arduino-based device with four DHT22 sensors was constructed for live monitoring of temperature and relative humidity during the experiment, as depicted in Figure 1b. An on-premises HVAC unit kept the laboratory and radiation room at 20 °C, which proved sufficient to maintain the samples at 20 ± 2 °C. The relative humidity in the climate chambers was above 90% during irradiation, and did not drop below 75% during penetration measurements. The relative humidity in the climate chambers was maintained by the evaporation of the layer of water present in the chambers. A heater and a nebulizer were considered for use, but proved unnecessary during the pre-experiment trials and equipment tests. The chamber with the lid in place is shown in Figure 2a, taken during the positioning of the target. Four molds filled with FA paste in position above the water in the climate chamber, with a DHT22 sensor visible, without the polystyrene lid, photographed during mix design optimization, and testing of the equipment and procedure (preparation for the irradiation experiment), are presented in Figure 2b.



(**a**) (**b**)

Figure 2. (**a**) Positioning of target in irradiation field; (**b**) samples placed above water surface, with humidity and temperature sensor visible on case wall.

Irradiation of the setting paste was performed at the "Vinča" Institute of Nuclear Sciences. The paste was prepared by vigorously mixing the powder and activator in a stainless steel vessel, using an electric mixer, for 5 min. Fresh paste was cast into cylindrical molds (40 mm in height, upper diameter 80 mm, lower diameter 70 mm) and manually tapped. The experiment/control sample pair for each material (BFS, MIX, and FA) was cast from the same batch. The sample to be irradiated was placed in the climate chamber and positioned in the irradiation field, as depicted in Figure 1a. The control sample was placed in the second climate chamber, and was placed in the laboratory outside the irradiation room, in an area serviced by the same HVAC system and away from direct sunlight. Both the laboratory and the irradiation room atmosphere were monitored using on-premises hygrometers and thermometers, and DHT22 sensors connected to an Arduino device. The temperature and humidity inside the climate chambers were continually monitored by DHT22 sensors connected to the Arduino device. For irradiation, the Co-60 reference field "IRPIK B" device was used at the Secondary Standard Dosimetry Laboratory (SSDL). The irradiation protocol is given in Table 4.

Table 4. Irradiation protocol.

Dose ($D_{air} \times t$) [Gy]	t [h]	D_{air} [Gy/h]	
8.02	50 min	9.62	BFS
17.54	1 h 50 min	9.569	MIX
34.14	3 h 35 min	9.528	FA

Using the SRPS EN 196-3:2017 standard as the guideline, the initial and final setting times were determined by measuring the penetration of the Vicat needle into the setting paste [31]. The criterion for the initial setting time was penetration of 6 mm or less, and for the final setting time, penetration of 1 mm or less. The procedure aimed to reduce the time between measuring the irradiated and control pastes to less than 5 min apart, with most pairs of measurements happening within 2 min. For the irradiated paste, irradiation was interrupted by lowering the radiation source; the time was noted on the irradiation device and manually; and the researcher entered the irradiation room and manually removed the climate chamber lid, positioned the Vicat carrier/bridge, took several penetration measurements and noted the time, removed the carrier/bridge, and repositioned the lid. As soon as researcher left the irradiation room, the source was lifted and irradiation continued, with the time noted on the IRPIK-B device control panel, and manually. Measurement of the control paste was performed in the same manner—removing the lid, taking several

penetration measurements, noting the time, and repositioning the lid, either right before or right after measuring the irradiated paste. Once the initial setting was observed, the circular mold was quickly and carefully sheared off the base plate, flipped, and repositioned back on the base plate. The final setting was determined by measuring the penetration of the collared Vicat needle—once the imprint of the collar was not observed on the paste surface, penetration was less than 1 mm, and the final setting time was noted.

3. Results

The initial and final setting times for the irradiated and control pastes are presented in Figure 3. The measured initial setting time was 45 min for irradiated BFS (1 h 11 min for the control), 1 h 57 min for MIX (1 h 55 min for the control), and 3 h 28 min for FA (3 h 27 min for the control). The final setting time was 1 h 10 min for irradiated BFS (1 h 14 min for the control), 2 h 12 min for MIX (2 h 13 min for the control), and 4 h 1 min for FA (4 h 20 min for the control). Irradiation led to shortening of the initial setting time for BFS, showed no notable effect for MIX, and led to shortening of the final setting time, but not the initial setting time, for FA.

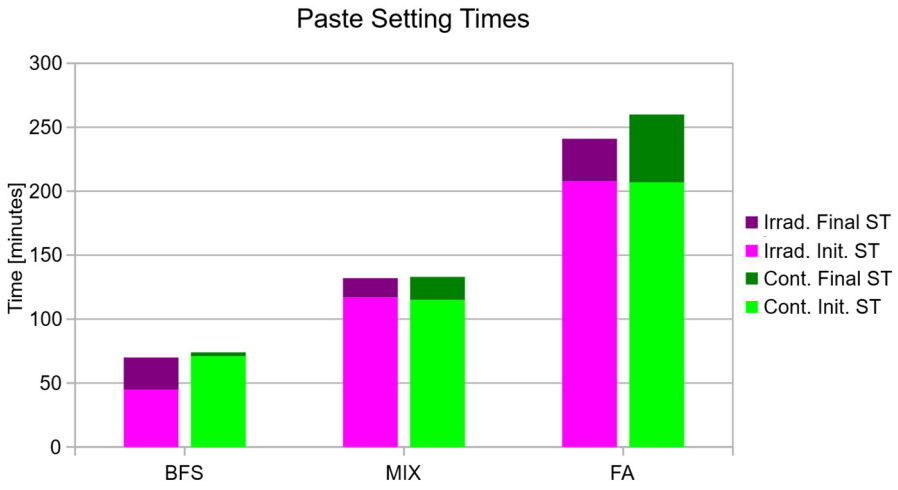


Figure 3. Setting times (ST) for BFS, MIX, and FA paste.

4. Discussion

The dose rate used in the irradiation of the samples, in the range of 9.5–9.6 Gy/h, is orders of magnitude lower than the dose rates used when long-term effects are studied, but far exceed the mean dose rates on the surface of the L/ILW containers, reported as reaching up to 0.002 Gy/h by Molnár et al. [32]. Irradiation was stopped once the binder had set, so BFS received the lowest total dose, MIX received more than double the dose received by BFS, and the FA binder received over four times the dose. Given the relatively low dose rates, and the fact that irradiated samples were kept under a controlled temperature, a thermal effect of irradiation can be excluded. If there was a thermal effect present, it would be expected that a reduction in setting times would be observed in all three mixtures. If the effect is based on the initial phase of alkali activation—the partial dissolution of solids in a strong base—the irradiated samples are expected to show a reduction in both the initial and the final setting times. Reactive oxygen species can lead to the formation and precipitation of new chemical species. It is plausible that ionizing radiation affects the processes differently, leading to the formation of C-A-S-H and N-A-S-H gel, and that those effects evened out during the irradiation of the 50:50 BFS/FA mix by weight. In this experiment, the previously reported shortening of the initial setting time for the FA binder was not observed [26].

For dose rates in the 9–10 Gy/h range, the irradiation by Co-60 gamma rays during setting did not lead to flash, nor did it delay the setting of the alkali-activated binder pastes. The effects on the initial and final setting times were either trivial or observable as shortening of the initial setting time for BFS and final setting time for the FA binder, all within the practical limits of fitness for purpose. These findings indicate that alkali-activated binders produced from industrial by-products can safely be used as an alternative to Portland cement in low- to intermediate-level radioactive waste encapsulation, given that chemical interactions of the waste and the cement matrix are accounted for.

Author Contributions: Conceptualization, L.R., S.S. and A.J.; Investigation, L.R. and S.S.; Methodology, L.R. and S.S.; Supervision, A.J.; Writing—Original Draft, L.R.; Writing—Review and Editing, S.S. and A.J. All authors have read and agreed to the published version of the manuscript.

Funding: This research was funded by the Ministry of Science, Technological Development and Innovation, Republic of Serbia, contract no. 451-03-66/2024-03/200051.

Data Availability Statement: The raw data supporting the conclusions of this article will be made available by the authors on request.

Acknowledgments: The authors express their gratitude to the Elektroprivreda Srbije (TENT branch) and HBIS Group Serbia corporations for providing the raw materials.

Conflicts of Interest: The authors declare no conflicts of interest.

References

1. Lee, W.E.; Ojovan, M.I. Fundamentals of Radioactive Waste (RAW): Science, Sources, Classification and Management Strategies. In *Radioactive Waste Management and Contaminated Site Clean-Up*; Elsevier: Amsterdam, The Netherlands, 2013; pp. 3–49, 50e, ISBN 978-0-85709-435-3.
2. Glasser, F. Application of Inorganic Cements to the Conditioning and Immobilisation of Radioactive Wastes. In *Handbook of Advanced Radioactive Waste Conditioning Technologies*; Elsevier: Amsterdam, The Netherlands, 2011; pp. 67–135, ISBN 978-1-84569-626-9.
3. Ukritnukun, S.; Sorrell, C.C.; Gregg, D.; Vance, E.R.; Koshy, P. Potential Use of Ambient-Cured Geopolymers for Intermediate Level Nuclear Waste Storage. *MRS Adv.* **2018**, *3*, 1123–1131. [CrossRef]
4. Garcia-Lodeiro, I.; Palomo, A.; Fernández-Jiménez, A. An Overview of the Chemistry of Alkali-Activated Cement-Based Binders. In *Handbook of Alkali-Activated Cements, Mortars and Concretes*; Elsevier: Amsterdam, The Netherlands, 2015; pp. 19–47, ISBN 978-1-78242-276-1.
5. Rakhimova, N. Recent Advances in Alternative Cementitious Materials for Nuclear Waste Immobilization: A Review. *Sustainability* **2022**, *15*, 689. [CrossRef]
6. Provis, J.L.; Van Deventer, J.S.J. Introduction to Geopolymers. In *Geopolymers*; Elsevier: Amsterdam, The Netherlands, 2009; pp. 1–11, ISBN 978-1-84569-449-4.
7. Zhong, Q.; Su, M.; Tian, X.; Peng, H. Workability and Mechanical Properties for GGBFS–MK Geopolymer Synthesis: Influencing Factor Analysis and a Mix Design Method. *Mater. Struct.* **2023**, *56*, 144. [CrossRef]
8. Reches, Y. A Multi-Scale Review of the Effects of Gamma Radiation on Concrete. *Results Mater.* **2019**, *2*, 100039. [CrossRef]
9. Bouniol, P.; Aspart, A. Disappearance of Oxygen in Concrete under Irradiation: The Role of Peroxides in Radiolysis. *Cem. Concr. Res.* **1998**, *28*, 1669–1681. [CrossRef]
10. Mobasher, N.; Bernal, S.A.; Kinoshita, H.; Sharrad, C.A.; Provis, J.L. Gamma Irradiation Resistance of an Early Age Slag-Blended Cement Matrix for Nuclear Waste Encapsulation. *J. Mater. Res.* **2015**, *30*, 1563–1571. [CrossRef]
11. Bouniol, P.; Muzeau, B.; Dauvois, V. Experimental Evidence of the Influence of Iron on Pore Water Radiolysis in Cement-Based Materials. *J. Nucl. Mater.* **2013**, *437*, 208–215. [CrossRef]
12. Cantarel, V. *Geopolymers and Their Potential Applications in the Nuclear Waste Management Field—A Bibliographical Study*; Japan Atomic Energy Agency: Ibaraki, Japan, 2017.
13. Phillip, E.; Choo, T.F.; Khairuddin, N.W.A.; Abdel Rahman, R.O. On the Sustainable Utilization of Geopolymers for Safe Management of Radioactive Waste: A Review. *Sustainability* **2023**, *15*, 1117. [CrossRef]
14. Rooses, A.; Steins, P.; Dannoux-Papin, A.; Lambertin, D.; Poulesquen, A.; Frizon, F. Encapsulation of Mg–Zr Alloy in Metakaolin-Based Geopolymer. *Appl. Clay Sci.* **2013**, *73*, 86–92. [CrossRef]
15. Lambertin, D.; Boher, C.; Dannoux-Papin, A.; Galliez, K.; Rooses, A.; Frizon, F. Influence of Gamma Ray Irradiation on Metakaolin Based Sodium Geopolymer. *J. Nucl. Mater.* **2013**, *443*, 311–315. [CrossRef]

16. Chupin, F.; Dannoux-Papin, A.; Ngono Ravache, Y.; d'Espinose De Lacaillerie, J.-B. Water Content and Porosity Effect on Hydrogen Radiolytic Yields of Geopolymers. *J. Nucl. Mater.* **2017**, *494*, 138–146. [CrossRef]
17. Geddes, D.A.; Walkley, B.; Galliard, C.L.; Hayes, M.; Bernal, S.A.; Provis, J.L. Effect of Exposure of Metakaolin-based Geopolymer Cements to Gamma Radiation. *J. Am. Ceram. Soc.* **2024**, *107*, 4621–4630. [CrossRef]
18. Yeoh, M.L.Y.; Ukritnukun, S.; Rawal, A.; Davies, J.; Kang, B.J.; Burrough, K.; Aly, Z.; Dayal, P.; Vance, E.R.; Gregg, D.J.; et al. Mechanistic Impacts of Long-Term Gamma Irradiation on Physicochemical, Structural, and Mechanical Stabilities of Radiation-Responsive Geopolymer Pastes. *J. Hazard. Mater.* **2021**, *407*, 124805. [CrossRef]
19. Li, Q.; Sun, Z.; Tao, D.; Xu, Y.; Li, P.; Cui, H.; Zhai, J. Immobilization of Simulated Radionuclide 133Cs+ by Fly Ash-Based Geopolymer. *J. Hazard. Mater.* **2013**, *262*, 325–331. [CrossRef] [PubMed]
20. Xu, Z.; Jiang, Z.; Wu, D.; Peng, X.; Xu, Y.; Li, N.; Qi, Y.; Li, P. Immobilization of Strontium-Loaded Zeolite A by Metakaolin Based-Geopolymer. *Ceram. Int.* **2017**, *43*, 4434–4439. [CrossRef]
21. Nikezić, D.; Janićijević, A. Bulk Etching Rate of LR115 Detectors. *Appl. Radiat. Isot.* **2002**, *57*, 275–278. [CrossRef]
22. Jantzen, C.M.; Lee, W.E.; Ojovan, M.I. Radioactive Waste (RAW) Conditioning, Immobilization, and Encapsulation Processes and Technologies: Overview and Advances. In *Radioactive Waste Management and Contaminated Site Clean-Up*; Elsevier: Amsterdam, The Netherlands, 2013; pp. 171–272, ISBN 978-0-85709-435-3.
23. Vance, E.R.; Perera, D.S. Development of Geopolymers for Nuclear Waste Immobilisation. In *Handbook of Advanced Radioactive Waste Conditioning Technologies*; Elsevier: Amsterdam, The Netherlands, 2011; pp. 207–229, ISBN 978-1-84569-626-9.
24. Komljenović, M.; Tanasijević, G.; Džunuzović, N.; Provis, J.L. Immobilization of Cesium with Alkali-Activated Blast Furnace Slag. *J. Hazard. Mater.* **2020**, *388*, 121765. [CrossRef]
25. Poulesquen, A.; Frizon, F.; Lambertin, D. Rheological Behavior of Alkali-Activated Metakaolin During Geopolymerization. In *Cement-Based Materials for Nuclear Waste Storage*; Bart, F., Cau-di-Coumes, C., Frizon, F., Lorente, S., Eds.; Springer: New York, NY, USA, 2013; pp. 225–238, ISBN 978-1-4614-3444-3.
26. Rubinjoni, L.; Stankovic, S.; Loncar, B. The Effect of 60Co Gamma Irradiation on Coal Fly-Ash Geopolymer Paste Setting Time. *Nucl. Technol. Radiat. Prot.* **2020**, *35*, 150–153. [CrossRef]
27. Janković, K.; Stanković, S.; Bojović, D.; Stojanović, M.; Antić, L. The Influence of Nano-Silica and Barite Aggregate on Properties of Ultra High Performance Concrete. *Constr. Build. Mater.* **2016**, *126*, 147–156. [CrossRef]
28. Nowakowski, B. Influence of Penetrating Ionizing Radiation on the Curing of Grouts and Cement Mortars. *Build. Sci.* **1972**, *7*, 271–276. [CrossRef]
29. Nowakowski, B. Admixtures of Irradiated Nuclei of Crystals and Their Influence upon the Hardening of Plain Cement. *Build. Sci.* **1972**, *7*, 277–285. [CrossRef]
30. Rubinjoni, L.; Stanković, S.; Janićijević, A. Measuring Geopolymer Set Times under Ionizing Radiation—Advances in Instruments and Procedures. In Proceedings of the International Conference IcETRAN, East Sarajevo, Bosnia and Herzegovina, 5–8 June 2023; Society for ETRAN: East Sarajevo, Bosnia and Herzegovina, 2023.
31. *SRPS EN 196-3:2017*; Methods of Testing Cement—Part 3: Determination of Setting Times and Soundness. Institut Za Standardizaciju Srbije: Belgrade, Serbia, 2017.
32. Molnár, M.; Palcsu, L.; Futó, I.; Svingor, É.; Major, Z.; Veres, M.; Ormai, P.; Barnabás, I. Study of Gas Generation in Real L/ILW Containers. *J. Radioanal. Nucl. Chem.* **2010**, *286*, 745–750. [CrossRef]

Disclaimer/Publisher's Note: The statements, opinions and data contained in all publications are solely those of the individual author(s) and contributor(s) and not of MDPI and/or the editor(s). MDPI and/or the editor(s) disclaim responsibility for any injury to people or property resulting from any ideas, methods, instructions or products referred to in the content.